

## Perpendicular magnetic anisotropy of binary alloys: A total-energy calculation

I. Galanakis, M. Alouani, and H. Dreysse

*IPCMS-GEMME, UMR CNRS-ULP 7504, 23, rue du Loess, F-67037 Strasbourg Cedex, France*

(Received 20 December 1999; revised manuscript received 14 January 2000)

Using the state-of-the-art relativistic full-potential version of the linear-muffin-tin orbital method we have performed *ab initio* calculations to study the magnetic properties of eight transition-metal binary alloys (FePt, CoPt, FePd, FeAu, MnPt<sub>3</sub>, CoPt<sub>3</sub>, VAu<sub>4</sub>, and MnAu<sub>4</sub>). Both the local-spin-density approximation (LSDA) and the generalized gradient approximation (GGA) to the exchange-correlation potential are used in the computation. The resulting spin and orbital magnetic moments of both approximations are similar and agree nicely with experiment, however, different values are found for the magnetocrystalline anisotropy energy (MCA), especially for MnPt<sub>3</sub>, CoPt<sub>3</sub>, and MnAu<sub>4</sub>. For all the other alloys the difference between the MCA values calculated within LSDA and GGA is less than 1 meV. The volume shape anisotropy is found to be important for the FePd and MnPt<sub>3</sub> thick films, while it is negligible for the other binary alloys.

### I. INTRODUCTION

Magnetic films with strong perpendicular magnetic anisotropy (PMA) are greatly attractive and promising for magneto-optical recording devices. Recently, a number of chemically ordered binary *d*-metal layered systems with perpendicular magnetization have been elaborated.<sup>1</sup>

The interpretation of the magnetic anisotropy energy (MAE) is a difficult task because it involves a small change in the total energy of the order of the  $\mu\text{eV}$  to the meV at the most, and it was shown<sup>2</sup> that not only states in the vicinity of the Fermi surface contribute to the MAE, but states far away make an equally important contribution. In the case of films the calculation of the MAE is an even more difficult task due to the low dimensionality. In 1988, Draaisma and de Longe described the MAE of one-element unsupported film making use of its structure but did not take into account physical effects like the interlayer interaction.<sup>3</sup> For enough thick films we can consider that the MAE does not depend on the substrate and the film has the same properties with an unsupported film with the same lattice parameters.

The early phenomenological model of Néel<sup>4</sup> for analyzing the MAE of magnetic films is still widely applied to interpret experimental data. In this model three major contributions are taken into account: (1) the magnetocrystalline anisotropy (MCA) arising principally from the spin-orbit interaction, which is a bulk property, the contribution of the magnetic dipole interactions to MCA is negligible;<sup>5</sup> (2) the volume shape anisotropy (VSA) due to magnetic dipole interactions that favors always an in-plane orientation of the magnetization axis, and (3) the so-called magnetosurface anisotropy (MSA) due to the low dimension of the surface geometry to which both spin-orbit coupling and dipole-dipole interactions contribute. The MSA decreases with the thickness of the film and for a film that is thick enough it is negligible compared to MCA. On the other hand the MCA for *3d* ferromagnets is of the order of  $\mu\text{eV}$  while for binary alloys it is of the order of meV. For binary alloys presenting PMA, the MCA is much larger than VSA and so the MAE of these films can be more suitably described using bulk calculations.

In addition, the disorder might also affect the MCA re-

sults as was shown by Razee *et al.* in the case of the  $\text{Co}_{1-x}\text{Pt}_x$  compounds using a fully-relativistic version of the Korringa-Kohn-Rostocker method in conjunction with the coherent potential approximation.<sup>6</sup> For the disordered  $\text{Co}_{1-x}\text{Pt}_x$  fcc compound the easy magnetization axis is along the [111] direction for all Pt concentrations and the calculated MCA decreases with temperature.<sup>6,7</sup> It was also shown that different ordering can change both the value of the MCA and the direction of the easy magnetization axis.<sup>8</sup> They compared their results on the MCA for the  $\text{Ni}_{1-x}\text{Pt}_x$  compound up to 25% concentration of Pt atoms with available experiments and showed that the calculated MCA follows the behavior of the experimental data.<sup>7</sup> Finally it is worth mentioning that the calculated MCA at  $T=0$  K in the case of the disordered fcc CoPt is only  $3.0 \mu\text{eV}$ ,<sup>6</sup> three orders of magnitudes smaller than both the calculated and the experimental MCA in the case of the ordered CoPt alloy.<sup>9</sup> The large MCA in the case of the ordered compound is due to the combined effect of the tetragonalization and atomic ordering.

Bruno formulated a relation that connects the orbital moment anisotropy to the MCA in the case of the *3d* transition metals.<sup>10</sup> This approach becomes valid only for systems where there are no holes in the spin-up band and the crystalline field parameter is much smaller than the spin-orbit coupling. Van der Laan generalized this approach to the case where holes are also present in the spin-up band.<sup>11</sup> Nevertheless, a relation that strictly relates the MCA, or more generally the MAE, to the orbital moments is not yet developed, and so the discussion for low-dimension systems like films or surfaces, is only valid at the qualitative level.

In this contribution we address the question of whether electronic structure calculations for bulk materials could be used to describe the magnetic properties of such thick films of binary alloys presenting PMA. Our calculation of the MAE is based on the determination of the total energy, using a *relativistic* linear muffin-tin orbital method,<sup>12</sup> so that the spin-orbit coupling originated MCA is implicitly included. Nevertheless, we do not take into account the explicit many-body interaction of spin magnetic moments<sup>13</sup> but this contribution, as mentioned above, has negligible contribution to the MCA. We will use a phenomenological model to esti-

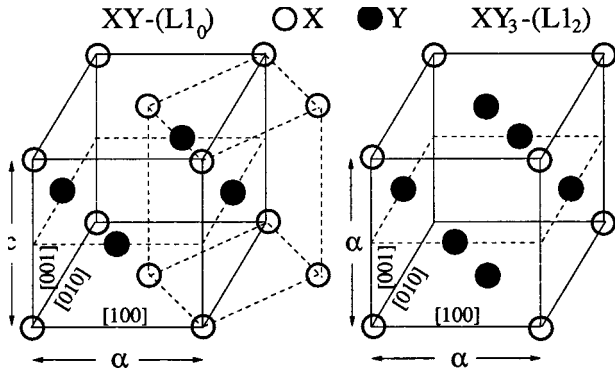


FIG. 1. Schematic representation of the  $L1_0$  and  $L1_2$  structures. Note that the  $L1_0$  along the  $[001]$  and the  $[110]$  directions and the  $L1_2$  structure along the  $[111]$  direction can be viewed as consisting of alternating layers of pure X and Y atoms. The  $L1_0$  presents high-uniaxial anisotropy contrary to the  $L1_2$ .

mate the VSA for thick films and compare experimental MAE results on films with calculated values. We have also calculated the magnetic moments and especially the anisotropy of the orbital moments, that is intrinsically correlated to the MAE.

To test the sensitivity of the MCA to the different treatments of the correlation effects of the Kohn-Sham equations,<sup>14</sup> we have used both the local-spin-density approximation (LSDA)<sup>15</sup> and the generalized gradient approximation (GGA)<sup>16</sup> to approximate the exchange-correlation potential. To our knowledge, this is the first study that checks both the LSDA and GGA for the computation of the MCA.

## II. DETAILS OF THE CALCULATIONS

We studied four systems that crystallize in the  $L1_0$  structure (see Fig. 1): FePt, FeAu, CoPt, and FePd. In Table I we have gathered the experimental lattice parameters in Å for all the systems (Ref. 17 for FePt, Ref. 18 for FeAu, Ref. 9 for CoPt, and Refs. 17 and 19 for FePd). For FePd we performed calculations using two different sets of lattice parameters, one set obtained by Kamp *et al.*,<sup>19</sup> which corresponds to a film of FePd grown on top of a MgO(001) substrate at 623 K that we denote as FePd(1), and second the parameters found in the book of Villars and Calvet<sup>17</sup> that we denote as FePd(2). The second group of systems consists of the CoPt<sub>3</sub> and MnPt<sub>3</sub> alloys, which are the only systems of the XPt<sub>3</sub> family that are collinear ferromagnets.<sup>20,21</sup> Figure 1 shows the  $L1_2$  structure of CoPt<sub>3</sub> and MnPt<sub>3</sub>; the bravais lattice is a simple cubic with the X atoms at the corners and the Pt atoms on the center of the faces. Most of the experimental work done for the XPt<sub>3</sub> compounds concerns films grown

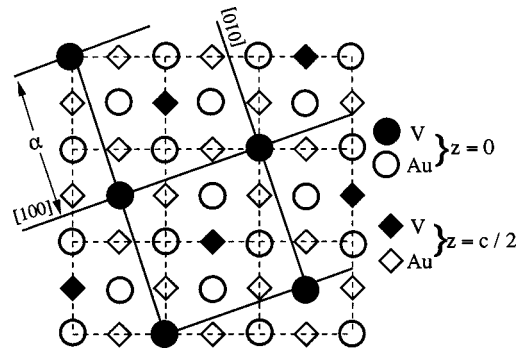


FIG. 2. The  $VAu_4$  and the  $MnAu_4$  adopt the  $Ni_4Mo$  structure. The vanadium or the manganese atoms occupy the positions of a body-centered-tetragonal structure with four gold atoms around each one of them. With circles we represent the atoms at the  $z=0$  layer and with diamonds the  $z=c/2$  layer. The  $c/a$  ratio is 0.624 for  $VAu_4$  and 0.625 for  $MnAu_4$  very close to the ideal one for which each vanadium or manganese atom would have 12 equidistant gold atoms as first neighbors. Notice that among the next-nearest neighbors only two are vanadium or manganese atoms.

along the  $[111]$  axis. These samples can present PMA when the spin align along the  $[111]$  direction. The in-plane  $[1\bar{1}0]$  direction in the case of films is equivalent to the  $[110]$  direction in our bulk calculations. The lattice parameters used in our calculations for these two systems are measured by Lange *et al.*,<sup>22</sup>  $a=3.857$  Å for CoPt<sub>3</sub> and 3.910 Å for MnPt<sub>3</sub>. Finally the  $VAu_4$  and  $MnAu_4$  systems crystallize in the  $Ni_4Mo$  crystal structure (see Fig. 2).<sup>23</sup>

To compute the magnetic properties of these systems we use the relativistic full-potential linear muffin-tin orbital (FP-LMTO) method.<sup>12</sup> Because of the hybrid nature of the basis set of this method the space is divided in two regions: (1) the nonoverlapping muffin-tin spheres centered at each atom and (2) the interstitial region. The muffin-tin potential is developed over the lattice harmonics of the system and the rest of the potential is treated using fast Fourier transform. The core electrons are spin polarized and their electronic states are obtained by solving the Dirac equation at each iteration of the self-consistent loop. Whereas for the valence electrons the Dirac Hamiltonian is expanded in first order of  $1/c^2$  ( $c$  being the speed of light), so that the total Hamiltonian including the Darwin and kinetic-energy corrections, as well as the spin-orbit coupling, is solved self-consistently. As stated in the Introduction, we use both the local-spin-density approximation<sup>15</sup> (LSDA) and the generalized gradient approximation<sup>16</sup> (GGA) to the exchange-correlation potential of the Kohn-Sham equations.<sup>14</sup> The GGA is a rather new functional and it has not been thoroughly tested for calculating very sensitive properties like the MCA. In this

TABLE I. Structure and experimental lattice parameters for all the studied binary alloys. Values are from Ref. 17 for FePt and FePd(2), Ref. 9 for CoPt, Ref. 19 for FePd(1), Ref. 18 for FeAu, and Ref. 22 for CoPt<sub>3</sub> and MnPt<sub>3</sub>. The  $VAu_4$  and  $Mn_4$  lattice parameters are quoted in the Ref. 43.

	$VAu_4$	$MnPt_3$	$MnAu_4$	FePd(1)	FePd(2)	FePt	FeAu	CoPt	CoPt <sub>3</sub>
Structure	$Ni_4Mo$	$L1_2$	$Ni_4Mo$	$L1_0$	$L1_0$	$L1_0$	$L1_0$	$L1_0$	$L1_2$
$a$ (Å)	6.382	3.910	6.45	3.89	3.860	3.861	4.08	3.806	3.857
$c/a$	0.624	1.0	0.625	0.938	0.968	0.981	0.939	0.968	1.0

paper we compute the MCA in both approximation and compare the results with experimental data whenever available.

MCA calculations strongly depend on the number of  $\mathbf{k}$  points for performing the Brillouin-zone (BZ) integration. The number of  $\mathbf{k}$  points needed to converge the value of the MCA depends strongly on the interplay between the contributions to the MCA from the Fermi surface and the remaining band-structure contribution to the total energy.<sup>24</sup> When the former contribution to the MCA is important, a large number of  $\mathbf{k}$  points is needed to describe accurately the Fermi surface. For the CoPt, FePt, FePd, and FeAu systems we found that 6750  $\mathbf{k}$  points in the BZ are enough to converge the MCA within 0.01–0.1 meV. For the CoPt<sub>3</sub> and MnPt<sub>3</sub> compounds we used 4096  $\mathbf{k}$  points and for the VAu<sub>4</sub> and MnAu<sub>4</sub> compounds 1000  $\mathbf{k}$  points. To perform the integrals over the BZ we use a Gaussian broadening method that convolutes each discrete eigenvalue with a Gaussian function of width 0.1 eV. This method is known to lead to a fast and stable convergence of the spin and charge densities compared to the standard tetrahedron method.

To develop the potential inside the MT spheres we calculated a basis set of lattice harmonics including functions up to  $l=8$  except for the CoPt<sub>3</sub> and Mn<sub>3</sub> compounds where  $l=6$  is found to be enough because of the higher symmetry of the  $L1_2$  structure compared to the other two. To perform the FFT we used a real-space grid of  $16 \times 16 \times 20$  for the  $L1_0$  compounds, and a grid of  $32 \times 32 \times 32$  for all the others. For the  $L1_0$  and  $L1_2$  compounds we used a double set of basis functions, one set to describe the valence states and one for the unoccupied states. For the valence electrons we used a basis set containing  $3 \times s$ ,  $3 \times p$ , and  $2 \times d$  wave functions, and for the unoccupied states  $2 \times s$ ,  $2 \times p$ , and  $2 \times d$  wave functions. We used five different values for the kinetic-energy parameter in the interstitial region  $\kappa^2$  used to calculate the basis wave functions ( $\kappa^2 = -1.5$  Ry,  $-0.3$  Ry, and  $+0.5$  Ry for the valence electrons and  $\kappa^2 = -0.8$  Ry and  $+0.6$  Ry for the unoccupied states). In the case of MnAu<sub>4</sub> and VAu<sub>4</sub>, we used a basis set with  $2 \times s$ ,  $2 \times p$ , and  $2 \times d$  wave functions ( $\kappa^2 = -0.4$  Ry and  $+0.5$  Ry) to describe the valence electrons. We also treated the  $5p$  electrons of Au and the  $3s$  and  $3p$  electrons of V as semicore using two wave functions for each case with  $\kappa^2 = -1.3$  Ry and  $-0.9$  Ry.

### III. MAGNETIC ANISOTROPY ENERGY

As we have already mentioned the MAE for a thick film is the sum between the MCA and the VSA. The MCA is defined as the total-energy difference between the hard and the easy magnetization axis, and is directly calculated from

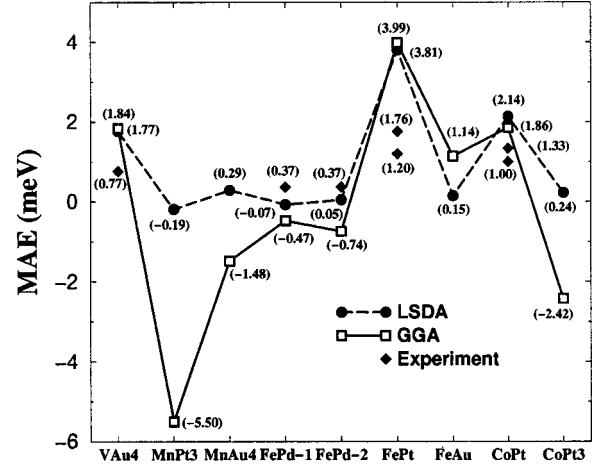


FIG. 3. XY, XPt<sub>3</sub>, and Mn(V)Au<sub>4</sub> thick films calculated MAE using both LSDA and GGA, as a sum of the calculated MCA and of the estimated VSA. The easy axis for the  $L1_0$  structure alloys and the V(Mn)Au<sub>4</sub> is the [001] and for XPt<sub>3</sub> the [111]. In the case of the FePt, CoPt, FeAu, and VAu<sub>4</sub> alloys the theory always favors the perpendicular axis. The other binary alloys show different behavior depending on the type of the approximation to the exchange-correlation potential. The experimental MAE results obtained by Kamp *et al.* (Ref. 19) for FePd, by Thiele *et al.* (Ref. 31) for FePt, by Eurin and Pauleve (Ref. 30) and Grange *et al.* (Ref. 9) for CoPt, and Adachi *et al.* (Ref. 50) for VAu<sub>4</sub> are presented with diamonds.

our *ab initio* results. For the  $L1_0$  systems the easy axis is along the [001] direction, the axis of film growth, whereas the hard axis is along the [100] direction. For the  $L1_2$  systems we define the [110] direction to be the hard axis and the [111] orientation to be the easy one. For VAu<sub>4</sub> and MnAu<sub>4</sub> we have the same definition as for the  $L1_0$  systems. A positive MCA or MAE value means that our calculation favors the easy magnetization axis. To compare our results with experiments on films, we have to estimate the VSA using the expression  $VSA = -2\pi M_V^2$  in cgs units, where  $M_V$  is the mean magnetization density, which can be obtained from the calculated spin magnetic moments.<sup>5</sup>

In Fig. 3 we present the calculated MAE for a thick-film structure within both LSDA and GGA and the available experimental results, and in Table II we have gathered the calculated MCA and VSA values. We can deduce directly from Fig. 3 that both LSDA and GGA produce the same tendencies as we pass from one system to another. But there are systems like MnPt<sub>3</sub>, CoPt<sub>3</sub>, and MnAu<sub>4</sub>, where the two functionals present strong deviations. For all the other binary alloys, the MCA values calculated within the two approximations differ less than 1 meV, but when the values are close

TABLE II. Estimated VSA and calculated MCA energies for the XY<sub>n</sub> binary alloys (X=V, Mn, Fe, or Co, and Y=Pt, Pd, or Au). In most cases, the VSA contribution to the MAE is smaller than the MCA. Except for FePd(1), VSA does not change the magnetization orientation with respect to the magnetization axis favored by the MCA.

	VAu <sub>4</sub>	MnPt <sub>3</sub>	MnAu <sub>4</sub>	FePd(1)	FePd(2)	FePt	FeAu	CoPt	CoPt <sub>3</sub>
VSA	-0.01	-0.09	-0.07	-0.13	-0.13	-0.10	-0.10	-0.06	-0.04
MCA-LSDA	1.78	-0.10	0.36	0.06	0.18	3.90	0.25	2.20	0.27
MCA-GGA	1.85	-5.41	-1.41	-0.34	-0.61	4.09	1.24	1.92	-2.38

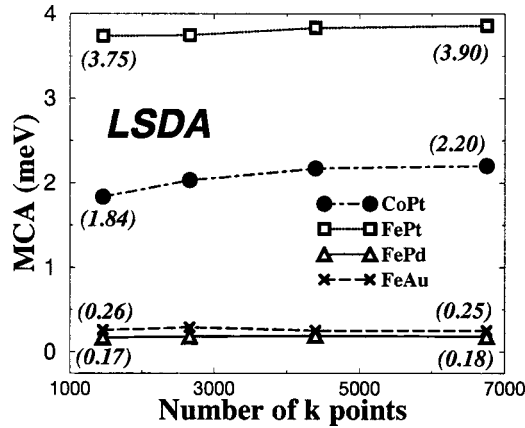


FIG. 4. Convergence of the MCA in meV with respect to the number of  $\mathbf{k}$  points in the Brillouin zone for the four  $L1_0$  compounds within LSDA. For FePd we present the result with the structure of FePd(2) (see Table I). We see that for all of them 6750  $\mathbf{k}$  points are enough to converge the MCA. Even for FePd and FeAu that present small values of MCA, the convergence is within 0.01 meV.

to zero, as is the case for FePd, it is possible that the LSDA and GGA predict a different magnetization axis.

#### A. FePt and CoPt

FePt and CoPt are the binary alloys that are the most studied both experimentally and theoretically. Our calculations for them show that the magnetization axis is indeed along the [001] direction and that the GGA and LSDA produce similar results for both systems. For FePt, LSDA produced a MCA value of 3.90 meV and GGA a value of 4.09 meV. For CoPt, LSDA and GGA produced values of 2.20 meV and 1.92 meV, respectively. In Fig. 4 we present the convergence with the number of  $\mathbf{k}$  points of all the binary alloys with the  $L1_0$  structure and within LSDA. We see that 6750 points are enough to converge within 0.1 meV.

These results are in good agreement with previous *ab initio* calculations by Solovyev *et al.*<sup>24</sup> using a real-space Green's function technique within the LSDA and treating the spin-orbit coupling as a perturbation (3.4 meV for FePt and 2.3 meV for CoPt). However, work by Sakuma<sup>25</sup> using the LMTO method in the atomic sphere approximation (ASA)<sup>26</sup> in conjunction with the force theorem<sup>27</sup> found slightly smaller values (2.8 meV for FePt and 1.5 meV for CoPt). Daalderop *et al.* found the values 2 meV for CoPt and 3.5 meV for FePt in agreement with our results. Oppeneer<sup>28</sup> used the augmented spherical wave method and found 2.8 meV for FePt and 1.0 meV for CoPt. Finally Ravindran *et al.*<sup>29</sup> found, using an earlier version of the code used also by us, 2.7 meV for FePt and 1.0 meV for CoPt. The value for CoPt is in perfect agreement with experimental values but experiments are carried out at room temperature. So theory should predict much larger values as is the case for our results. The discrepancy between the two calculations possibly arises from the basis set used in the calculations (Ravindran *et al.* used only 8 basis wave functions contrary to 14 in our calculations).

Our PMA values for CoPt are compared with the experimental results at ambient temperature of Eurin and Pauleve<sup>30</sup>

(1.3 meV), and of Grange *et al.*<sup>9</sup> (1.0 meV). Eurin's value is for a monocrystal of CoPt so this value can be directly compared to our calculations. Grange *et al.*'s experiment is on a film of CoPt. For CoPt the VSA is  $-0.06$  meV, which is two order of magnitudes smaller than the experimental MAE value, and hence it does not influence the magnetization orientation. In agreement with the theoretical finding, the experimental MAE value for FePt films of 1.76 meV is larger than the values for CoPt (see Fig. 3).<sup>31</sup> Ivanov *et al.* found for FePt a MCA value of 1.2 meV and predicted that VSA would be one order of magnitude smaller than MCA.<sup>32</sup> This is in agreement with our estimated value of VSA for FePt of  $-0.1$  meV (see Table II). Here again the VSA does not influence the magnetization orientation.

#### B. FePd and FeAu

FePd films are known to present different magnetic properties depending on the deposition conditions. We have chosen to calculate the magnetic properties for lattice parameters corresponding to a film grown by Kamp *et al.* at 623 K, because it is highly ordered (90% of the atoms were at the correct site),<sup>19</sup> which we denote as FePd(1) and for the structure given in the handbook of Villars and Calvet, which is used in all the other *ab initio* calculations cited in this section and we denote as FePd(2).<sup>17</sup> In this particular case both the LSDA and GGA produced about the same MCA values for both systems. The LSDA produced 0.06 meV for FePd(1) and 0.18 meV for FePd(2), while GGA produced  $-0.34$  meV and  $-0.61$  meV, respectively. Contrary to the other two compounds with the  $L1_0$  structure, the LSDA and GGA MCA values are in disagreement. GGA favors a different magnetization axis than LSDA. The absolute LSDA values are one order of magnitude smaller than the ones for the XPt compounds.

Previous calculations of Solovyev *et al.*<sup>24</sup> found a MCA value that varies from 0.1 meV to 0.3 meV depending on the treatment of the spin-orbit coupling in agreement with our LSDA values of 0.06 and 0.18 meV. Daalderop *et al.*<sup>33</sup> calculated a value of 0.51 meV using the LMTO-ASA in conjunction with the force theorem. Finally Oppeneer found a value of 0.55 meV,<sup>28</sup> and Ravindran *et al.* found a value of 0.15 meV for the same lattice parameters with FePd(2) and their value is very close to our value of 0.18 meV.<sup>29</sup> It is worth noticing that even methods that calculate total energies like ours and the one used by Oppeneer produce for FePd considerably different results underlining the sensitivity of the MCA not only to the density functional used but to the details of the *ab initio* method as well. Trends of the MCA for different systems convey more physics than the absolute values.

Kamp's MAE experimental value for a FePd thick film of 0.37 meV is larger than our calculated LSDA values. The VSA for a FePd film is  $-0.13$  meV in both cases, so that the total MAE for a FePd(1) thick film is  $-0.07$  meV, within the LSDA and  $-0.47$  meV, within the GGA, and both LSDA and GGA predict the wrong magnetization axis. In the case of FePd(2), the MAE within the LSDA is 0.05 meV and within the GGA is  $-0.74$  meV. The fact that the LSDA predicts the correct magnetization axis for the

TABLE III. Calculated spin magnetic moments within both the LSDA and GGA in units of  $\mu_B$  for the  $XY_n$  binary alloys ( $X=V, Mn, Fe, \text{ or } Co$ , and  $Y=Pt, Pd, \text{ or } Au$ ). The magnetism on Pt (Pd or Au) site is induced by the hybridization between the Fe (Co, or Mn)  $3d$  orbitals and the  $4d(5d)$  orbitals of Pd (Pt or Au). The vanadium and gold in their bulk forms are paramagnets but their binary alloy is a weak ferromagnet. All results except for the  $VAu_4$  and FePd agree nicely with the experimental data. The experimental results are taken from Ref. 17 for the FePt, Ref. 9 for the CoPt, Ref. 46 for the CoPt<sub>3</sub>, Ref. 47 for the MnPt<sub>3</sub>, Ref. 19 for the FePd(1), Ref. 39 for FePd(2), Ref. 18 for the FeAu, Ref. 50 for the  $VAu_4$ , and Ref. 51 for  $MnAu_4$ .

$\mu^{spin}$	X-LSDA	X-GGA	X-Exp	Y-LSDA	Y-GGA	Y-Exp
$VAu_4$	1.67	1.79	1.00	<0.01	>-0.01	
MnPt <sub>3</sub>	3.66	3.78	3.60	0.12	0.12	0.17
MnAu <sub>4</sub>	3.96	4.04	4.0	0.02	0.02	
FePd(1)	2.90	3.02	2.04	0.35	0.36	0.62
FePd(2)	2.96	3.02		0.35	0.34	0.4
FePt	2.88	2.96	2.80	0.33	0.34	
FeAu	2.95	3.00	2.75	0.05	0.04	
CoPt	1.74	1.83	1.76	0.35	0.37	0.35
CoPt <sub>3</sub>	1.82	1.89	1.64	0.22	0.24	0.26

FePd(2) thick film is relevant because the calculated MAE value of 0.05 meV is really small and is very sensitive to thermal effects.

In the case of the artificial alloy FeAu, both LSDA and GGA produce the same easy magnetization axis, the [001], and MCA values of about 0.25 and 1.24 meV, respectively. The estimated VSA is  $-0.10$  meV and is not enough to rotate the magnetization axis in-plane. These results agree with the experiments of Takanashi *et al.*<sup>18</sup> that also predicted the easy axis along the [001] direction. The MAE values for FeAu are larger than in the case of FePd but remain considerably smaller than the FePt values.

### C. MnPt<sub>3</sub> and CoPt<sub>3</sub>

For the MnPt<sub>3</sub> and CoPt<sub>3</sub> the situation is more complicated than the above binary alloys. The GGA favors the [110] axis and its MCA values are at least one order of magnitude larger than the LSDA values. In particular, for CoPt<sub>3</sub> the LSDA slightly favors the [111] axis while for MnPt<sub>3</sub> the [110]. In contrast, the GGA favors the in-plane axis for both systems. One plausible explanation for these conflicting results is that the GGA strongly favors one magnetization axis for all  $XPt_3$  materials. The GGA calculations should not be considered as an improvement over the LSDA, and only a good comparison with experiment for each system and property justifies its use instead of the LSDA. It seems then that in the case of these two alloys, and in the absence of experimental results, it is hard to justify either of the two approximations to the exchange-correlation potential. The only available experimental information<sup>34</sup> concerns CoPt<sub>3</sub> films grown along the [111] direction, where PMA is obtained for a certain range of temperatures. It is then highly desirable to study the temperature dependence of the MCA by extending our theory, which is now restricted to  $T=0$  K. The estimated VSA for these two compounds is  $-0.04$  meV for CoPt<sub>3</sub> and  $-0.1$  meV for MnPt<sub>3</sub>. The CoPt<sub>3</sub> VSA is weaker than the MCA values. The MnPt<sub>3</sub> VSA is comparable to the LSDA MCA value

( $-0.09$  meV). In this latter case the addition of the VSA to the MAE does not change its sign, and the magnetization remains in-plane (see Fig. 3).

### D. VAu<sub>4</sub> and MnAu<sub>4</sub>

The  $VAu_4$  compound is particularly interesting because it is the first ferromagnet, discovered in the sixties, which consists of elements that are paramagnetic in their bulk forms.  $MnAu_4$  is also known to be a ferromagnet.<sup>35</sup> Our LSDA and GGA calculations show that  $VAu_4$  presents a PMA assuming that the film growth is along the [001] direction, which indeed is the highest-symmetric axis. The GGA MCA is slightly larger compared to the LSDA (1.9 meV compared to 1.8 meV). The estimated VSA for a  $VAu_4$  thick film is about  $-0.01$  meV and is negligible compared to the MCA. The reason for such a weak VSA is that the four gold atoms carry practically no spin moment so that only the magnetism of the vanadium atom contributes to the average magnetization density.

In the case of  $MnAu_4$  things are more complex. LSDA still favors an out-of-plane axis (MCA=0.36 meV), but GGA favors an in-plane axis with a quite large value of MCA of  $-1.41$  meV. The estimated VSA is  $-0.07$  meV, and so it does not change the magnetization axis neither in the case of LSDA or GGA.

## IV. MAGNETIC MOMENTS

In this section we will present our calculated spin and orbital magnetic moments. Spin moments are insensitive with respect to the magnetization axis and in Table III we have gathered the values for all the systems within both approximations LSDA and GGA together with the experimental results. For all systems the LSDA and GGA produce similar results, so both functionals describe the spin magnetic moments with the same accuracy. The most important part of this section is the orbital moments because their anisotropy with respect to the magnetization axis is directly

TABLE IV. Orbital moments for both magnetization axis for all the binary alloys that crystallize in the  $L1_0$  structure. In all cases LSDA and GGA produce similar results, and hence the discrepancy in the MCA values whenever it occurs cannot be explained in terms of a different estimation of the orbital moment anisotropy between the two functionals. We also remark that the Pt, Pd, and Au atoms, although their small spin moment compared to Fe and Co, present comparable orbital moments, principally due to their large spin-orbit coupling.

$\mu^{orb}$	FePd(1)	FePd(2)	FePt	FeAu	CoPt
X-LSDA [001]	0.07	0.07	0.07	0.07	0.11
X-GGA [000]	0.07	0.07	0.07	0.06	0.09
X-LSDA [100]	0.06	0.07	0.07	0.05	0.06
X-GGA [100]	0.06	0.06	0.07	0.05	0.07
Y-LSDA [001]	0.03	0.03	0.05	0.03	0.06
Y-GGA [001]	0.03	0.03	0.05	0.03	0.06
Y-LSDA [100]	0.03	0.03	0.05	0.04	0.08
Y-GGA [100]	0.03	0.03	0.06	0.04	0.07

correlated to the MCA. In the part that follows we will present our results for each studied system.

### A. FePt and CoPt

Iron based alloys are strong ferromagnets and this is reflected on much higher spin magnetic moments compared to Co based alloys, as can be seen in Table III. The hybridization between Fe  $3d$  orbitals and Pt  $5d$  orbitals is much weaker than in the Co compounds leading to a smaller Pt induced spin magnetic moment in FePt. For the  $3d$  ferromagnets, the GGA is known to produce more atomiclike description compared to the LSDA, and as a consequence the resulting magnetic moments are slightly larger (see Table III). Nevertheless, we found it surprising that the GGA Pt spin moments are slightly larger than the corresponding LSDA values. It seems that the  $3d$  ferromagnetic moment increase leads to a stronger spin polarization of the Pt  $5d$  electrons, in spite of the decreasing hybridization caused by a more atomiclike description of the  $3d$  metal.

Our calculated magnetic moments are in excellent agreement with previous calculations using the LSDA by Sakuma,<sup>25</sup> Solovyev *et al.*,<sup>24</sup> Daalderop *et al.*,<sup>33</sup> Osterloh *et al.*,<sup>36</sup> and by Kootte *et al.*<sup>37</sup> for FePt and CoPt compounds. By comparing our results to the available experimental values by Villars and Calvet for FePt<sup>17</sup> and by Grange *et al.*<sup>9</sup> and Laar<sup>38</sup> for CoPt we see that both GGA and LSDA describe accurately the spin moments. It is however expected that a mean-field theory should overestimate slightly the experimental spin moments due to the neglect of spin fluctuations caused by thermal vectors and because the measured moments are the projections of the total spin moments on the magnetization axis.

In Table IV we have gathered the orbital moments for all the  $L1_0$  type binary alloys within both approximations and for both the hard and easy magnetization axis. The orbital moment anisotropy is more important in the case of cobalt than in the case of Fe in FePt. The LSDA cobalt orbital moment changes by  $0.048 \mu_B$  and the GGA moment by  $0.027 \mu_B$  as we pass from the easy axis [001] to the hard axis [100]. The LSDA iron moment changes by  $0.002 \mu_B$  and the GGA moment is the same for the two high-symmetry directions. We see that the GGA produces larger moments

than the LSDA for platinum in FePt contrary to CoPt. The platinum moments are in general smaller than the moments of the  $3d$  ferromagnets, and the difference between the values calculated within LSDA and GGA are small. The absolute values for platinum are comparable to cobalt(iron) orbital moments even though the spin moments on platinum are one order of magnitude smaller than for cobalt(iron). The large orbital moments for platinum are due to a much larger spin-orbit coupling for the  $d$  electrons of the platinum compared to the  $3d$  ferromagnets.

The orbital moments of FePt and CoPt have been previously calculated by Oppeneer<sup>28</sup> for both magnetization axis, and by Daalderop and collaborators<sup>33</sup> and Solovyev and collaborators<sup>24</sup> for the [001] direction using the LSDA. The  $L1_0$  structure is close packed and we expect the ASA to perform as well as our full-potential method. Oppeneer used the LMTO-ASA method and found values slightly larger than ours but the orbital moment anisotropy is similar to ours for both FePt and CoPt compounds. The orbital moment of the cobalt site was found to be  $0.12 \mu_B$  by Daalderop and  $0.09 \mu_B$  by Solovyev. The value of Daalderop is closer to our LSDA value of  $0.11 \mu_B$ . For the iron site, Daalderop found a value of  $0.08 \mu_B$  and Solovyev  $0.07 \mu_B$ , in good agreement with our LSDA value. The platinum orbitals moments have been calculated by Solovyev. He found a value of  $0.06 \mu_B$  for platinum in CoPt and  $0.044 \mu_B$  for platinum in FePt, close to our values of  $0.06 \mu_B$  and  $0.05 \mu_B$ , respectively.

### B. FePd and FeAu

Fe spin moments in FePd and FeAu compounds show the same behavior as in FePt. Fe spin magnetic moments in both compounds are larger than for the Fe atom in FePt leading to a larger polarization of the Pd- $4d$  electrons and consequently to a larger Pd spin magnetic moment compared to the Pt atom (Pd has the same number of valence electrons as Pt). The Au atom has its valence  $d$  states filled contrary to Pd and Pt and consequently an induced spin magnetic moment that is one order of magnitude smaller than these of Pt and Pd. The GGA Fe spin moments are slightly larger than the LSDA values while the Pd and Au spin moments are practically the same for both functionals.

TABLE V. Our calculated spin and orbital moments for  $\text{CoPt}_3$  and  $\text{MnPt}_3$  compounds together with previous calculations using the LSDA by Oppeneer *et al.* (Ref. 44) (values between parentheses) using the LMTO-ASA and Kulatov *et al.* (Ref. 20) (values between accolades) using the relativistic ASW for the magnetization along the [111] direction. All *ab initio* results are in agreement except for the Pt orbital magnetic moments. For the [110] direction the three Pt atoms are inequivalent and so they have different orbital moments. The first value concerns the two Pt atoms with  $z = c/2$  (see Fig. 1) and the second value the Pt atom with  $z = 0$ .

	$\mu^{spin}$		X atom			Pt atom		
			$\mu^{orb}$ [111]	$\mu^{orb}$ [110]		$\mu^{orb}$ [111]	$\mu^{orb}$ [110]	
MnPt <sub>3</sub> -LSDA	(3.71) 3.66	(0.03) 0.03	0.03	0.03	(0.12) 0.12	(~0) -0.04	~0	-0.01
MnPt <sub>3</sub> -GGA	[3.70] 3.78	[0.03] 0.03	0.02	0.02	[0.12] 0.12	[~0] -0.04	~0	> -0.01
CoPt <sub>3</sub> -LSDA	(1.68) 1.82	(0.05) 0.04	0.04	0.04	(0.26) 0.22	(0.05) 0.02	~0	0.04
CoPt <sub>3</sub> -GGA	[1.80] 1.89	[0.07] 0.05	0.05	0.05	[0.24] 0.24	[0.05] 0.02	~0	0.05

Kamp's experimental spin magnetic moments for FePd differ considerably from our calculated values as can be seen in Table III.<sup>19</sup> From first sight, it seems that both approximations, LSDA and GGA, strongly underestimate the hybridization between the Fe-3*d* and the Pd-4*d* electrons, predicting larger Fe spin magnetic moments and smaller Pd ones. This is strange regarding both the experimental and theoretical results for the Pt-based compounds. We believe that the main reason for this discrepancy comes from the experiment. This point of view is strengthened by the fact that Kamp found surprisingly that the Fe magnetic moment for the disordered sample is much larger than for the ordered one. Cros *et al.* measured the XMCD at the Pd  $L_{2,3}$  edges and extracted a Pd spin magnetic moment of  $0.4 \mu_B$  in good agreement with our values.<sup>39</sup> Finally for the FeAu only the Fe spin moment has been measured and was found to be  $2.8 \mu_B$  close to our value of  $\sim 3.0 \mu_B$ .<sup>18</sup>

Orbital moments show the same behavior as in the case of FePt. Fe orbital moments are comparable in all Fe compounds, but in the case of FeAu they exhibit a larger anisotropy. The in-plane Fe orbital moments are smaller than the out-of-plane orbital magnetic moments, and the LSDA produces slightly larger values compared to the GGA. We remark that both orbital and spin moments present minor differences between the two FePd compounds, especially the Pd ones. Both the LSDA and GGA produce the same values of Pd orbital moments and, contrary to Fe moments, the in-plane values are larger. The Au orbital moments have the same behavior as the Pd ones, but the absolute values are larger than for the Pd atom, while they stay smaller than these of the Pt atoms. Globally both the GGA and LSDA produce a similar orbital moment anisotropy for both FePd and FeAu, thus we are unable to connect the difference of the MCA values obtained by using the two density functionals to that of the orbital moments.

Regarding the Fe site orbital moment in FePd, Kamp found it to be  $0.42 \pm 0.05 \mu_B$ ,<sup>19</sup> much higher than the calculated value. These experimental values are about five times larger than the values for the bulk bcc Fe. This difference is surprisingly large in spite of the fact that the orbital moment is mostly an atomic property. Cros *et al.*<sup>39</sup> applied the sum

rules and obtained an orbital moment of  $0.004 \mu_B$  for Pd site, about one order of magnitude smaller than our calculated values. But because the error on the values of the orbital moment obtained from the sum rules exceeds easily  $0.01 \mu_B$ , we believe that our result is in qualitative agreement with experiment.<sup>40</sup> No information on the experimental sample is available but we suspect that the discrepancy comes from the effect of the disorder in the sample and from the limited applicability of the sum rules to the 4*d* system.

As was the case for FePt and CoPt our calculated magnetic moments along the [001] direction are in agreement with previous calculations using the LSDA by Solovyev *et al.*,<sup>24</sup> Moruzzi and Marcus,<sup>41</sup> and Daalderop *et al.*<sup>33</sup> for FePd. Oppeneer used the LMTO-ASA method and obtained orbital moments for both magnetization axis of the FePd slightly larger than ours; but his orbital moment anisotropy is close to ours.<sup>28</sup> Concerning the FeAu compound, Nakata *et al.* calculated only the Fe spin moment and found a value of  $2.75 \mu_B$ , which is slightly smaller than ours.<sup>42</sup> Oppeneer calculated also the Fe and Au spin and orbital magnetic moments for a magnetization along the [001] direction by means of the ASW-ASA method.<sup>43</sup> His values are similar to ours with the exception of the orbital moment of Fe of  $0.09 \mu_B$  that is larger than our value by  $0.02 \mu_B$ .

### C. $\text{CoPt}_3$ and $\text{MnPt}_3$

Table III presents the calculated spin magnetic moments of the  $\text{CoPt}_3$  and  $\text{MnPt}_3$  compounds and in Table V we have also gathered the orbital moments. As was the case for the iron based compounds, manganese based alloys are strong ferromagnets and this is reflected on much larger spin magnetic moments compared to Co based alloys. The hybridization between Mn 3*d* orbitals and the Pt 5*d* orbitals is much weaker than in the Co compounds leading to a smaller Pt induced spin magnetic moment in  $\text{MnPt}_3$ . Especially in the case of  $\text{MnPt}_3$  where Mn spin moment is practically twice the spin moment of Co in  $\text{CoPt}_3$ , the induced spin moment at the Pt site is halved compared to that in  $\text{CoPt}_3$ . Co in  $\text{CoPt}_3$  is more atomiclike than in CoPt, which is reflected in slightly larger spin moment. Because the number of cobalt's Pt first

TABLE VI. Spin and orbital magnetic moments for the  $\text{MnAu}_4$  and the  $\text{VAu}_4$  systems. Vanadium atoms do not obey the Hund's 3rd rule. Both functionals produce similar values except for the V atom that LSDA predicts a larger orbital moments anisotropy compared to GGA.

	X atom			Au atom		
	$\mu^{spin}$	$\mu^{orb}$ [001]	$\mu^{orb}$ [100]	$\mu^{spin}$	$\mu^{orb}$ [001]	$\mu^{orb}$ [100]
$\text{VAu}_4$ -LSDA	1.67	0.16	0.06	<0.01	-0.01	-0.01
$\text{VAu}_4$ -GGA	1.79	0.08	0.05	<0.01	-0.01	-0.01
$\text{MnAu}_4$ -LSDA	3.96	-0.01	> -0.01	0.02	0.01	0.01
$\text{MnAu}_4$ -GGA	4.04	-0.01	> -0.01	0.02	0.01	0.01

neighbors is greater for  $\text{CoPt}_3$  than  $\text{CoPt}$ , the induced polarization of Pt  $5d$  orbitals in the former compound is much smaller than the latter one, leading to a 30% decrease in the spin magnetic moment.

Our calculated spin magnetic moments are in agreement with previous LSDA calculations.<sup>20,44,45</sup> Tohyama *et al.* calculated also the spin moments using a semiempirical method and overestimated the spin moments with respect to all the *ab initio* calculations.<sup>21</sup> By comparing our results to the available experimental values,<sup>46,47</sup> we notice that, the theory slightly underestimates the hybridization between the Mn(Co) and Pt  $d$  orbitals leading to slightly larger Co and Mn spin moments and slightly smaller Pt moments. A total moment of Mn of  $3.92 \mu_B$  has been measured by Lange *et al.*<sup>22</sup> for a polycrystalline powder, which is close to the value of  $3.9 \mu_B$  of a completely ordered sample measured by Auwärter and Kussman,<sup>48</sup> and slightly smaller than other experimental values measured by Pickart and Nathans<sup>47</sup> ( $4.11 \mu_B$ ) and Antonini *et al.*<sup>49</sup> ( $4.04 \mu_B$ ). Our calculated value of  $4.08 \mu_B$  agrees well with the experimental values. In the case of  $\text{CoPt}_3$ , Lange *et al.*<sup>22</sup> found for a polycrystalline powder a total Co moment of  $2.80 \mu_B$  larger than our LSDA value of  $2.48 \mu_B$  but Menzinger and Paoletti<sup>46</sup> found a value of  $2.42 \mu_B$  by neutron scattering for a completely ordered sample, much closer to ours.

The most important feature for these two compounds are the orbital moments as they may give a plausible explanation for the large discrepancies of the calculated MCA values using LSDA and GGA. Unfortunately no conclusions can be drawn. For both compounds, LSDA produces no orbital moment anisotropy for the Mn and Co atoms. In the case of  $\text{MnPt}_3$  the orbital moment for the [110] axis is practically zero for the two Pt atoms with  $z=c/2$ , while the Pt atom at  $z=0$  present an orbital moment that is one order of magnitude smaller than the value for the [111] axis. So along the [110] direction Pt orbital moments show a large anisotropy. In contrast the GGA produces for the Mn atom an anisotropy of  $0.01 \mu_B$  that is very small, and for the Co an anisotropy of  $0.07 \mu_B$ . For the Pt atom the GGA and LSDA produce similar results. So although both LSDA and GGA produce similar orbital magnetic anisotropy values for the Mn(Co) $\text{Pt}_3$  compounds they produce large discrepancies for the MCA, showing that the calculation of the MCA is a much more difficult and sensitive task than the calculation of the orbital moments.

In Table V we have gathered also the orbital moments calculated by Kulatov *et al.*<sup>20</sup> and Oppeneer *et al.*<sup>44</sup> In the case of the Co and Mn atoms, their calculations agree nicely with our results, especially for the Mn atom. For the Co atom they predict a larger orbital moment compared to our calculations. Discrepancies occur in the case of the Pt sites. For  $\text{MnPt}_3$  both calculations by Kulatov *et al.*<sup>20</sup> and by Oppeneer *et al.*<sup>44</sup> produce a practically zero moment contrary to our value of about  $-0.036 \mu_B$ . The tendency is reversed in the case of  $\text{CoPt}_3$  where they predicted a magnetic moment of about twice our value. Finally Iwashita *et al.* calculated also the orbital magnetic moments using the full-potential linear augmented plane wave (FLAPW) method.<sup>45</sup> Their calculated Pt orbital moments agree with the calculations of Kulatov *et al.*,<sup>20</sup> and Oppeneer *et al.*,<sup>44</sup> but their values of Mn and Co are practically zero contrary to all other *ab initio* results. This discrepancy can arise from the small number of  $\mathbf{k}$  points Iwashita *et al.* have used in their calculations (just 20  $\mathbf{k}$  points in the irreducible part of the first Brillouin zone).

#### D. $\text{VAu}_4$ and $\text{MnAu}_4$

As was the case for all the other alloys, both the LSDA and GGA spin magnetic moments are similar. Vanadium spin magnetic moments are much larger than the experimental value of  $1.0 \mu_B$ ,<sup>50</sup> and as it was the case for the other alloys the GGA overestimates the vanadium spin moment compared to the LSDA ( $1.79 \mu_B$  compared to  $1.67 \mu_B$ ). The gold site has a weak induced spin magnetic moment; its absolute value is less than  $0.01 \mu_B$ . As expected the manganese spin moment is more than twice the value of the vanadium one and slightly larger than in the case of  $\text{MnPt}_3$ . Experimentally the Mn spin magnetic moment was measured to be  $4.0 \mu_B$ , near both our LSDA and GGA values.<sup>51</sup> The larger Mn spin moment compared to the V one leads to a larger polarization of the Au  $d$  orbitals and thus to a larger Au spin moment of  $0.02 \mu_B$ .

In Table VI we have gathered the orbital moments for both compounds. For the magnetization axis along the [100] direction the four gold atoms are inequivalent and we give both orbital magnetic moments values. We see that LSDA and GGA produce different values of the orbital moments but both of them predict a large orbital moment anisotropy for the V atom, while in the case of the Mn atom the anisotropy is too small. What is astonishing is that V atoms do not

obey the third Hund's rule concerning the relative orientation of the spin and orbital magnetic moments. This can be explained in terms of the influence of the spin-orbit coupling of the Au ligand states.<sup>52</sup> LSDA produces larger Au orbital moments in the case of VAu<sub>4</sub>, while the situation is the opposite for MnAu<sub>4</sub>. As was the case for the other compounds differences in the orbital moment anisotropy calculated within LSDA and GGA cannot justify the different values of MCA for the MnAu<sub>4</sub> compound.

Previous calculations have been carried out by Kübler<sup>23</sup> for VAu<sub>4</sub> and by Oppeneer *et al.*<sup>43</sup> for both compounds. Both found large vanadium spin magnetic moments that agree with our value. Oppeneer calculated also the total moment for the Mn atom, 4.02  $\mu_B$ , that is larger than our LSDA value of 3.78  $\mu_B$ . Oppeneer *et al.*<sup>43</sup> have also calculated a total Au moment in VAu<sub>4</sub> of  $-0.006 \mu_B$  that agrees perfectly with our LSDA value of  $-0.007 \mu_B$  when the magnetization is along the [001] direction.

## V. CONCLUSIONS

We showed that the full-potential linear muffin-tin orbital method within either the LSDA or the GGA to the exchange-correlation potential describes accurately the spin and orbital magnetic moments. Nevertheless, these two approximations produced different results for the MCA energy. In particular, while for FePt, CoPt, FeAu, and VAu<sub>4</sub> the LSDA and GGA results seem to be consistent, it is not the case for the other binary alloys where the discrepancy between the two approximations is at the qualitative level. For FePd, the LSDA produced a positive MCA, and the MAE becomes slightly negative when the volume contribution to the shape anisotropy

is added to the MCA. Consequently, for bulk FePd the LSDA predicts PMA while GGA predicts an in-plane magnetization, but for thick films both methods produced an in-plane magnetization axis. For the XPt<sub>3</sub> and MnAu<sub>4</sub> compounds the lack of experimental evidence does not allow us to decide whether LSDA or GGA is more adequate for the computation of the MCA. Finally we estimated the volume contribution to the shape anisotropy for a thick film and found that it is important compared to our calculated MCA values in the case of FePd and MnPt<sub>3</sub>. For the other six compounds this contribution to the MAE is much weaker than the MCA, and hence it plays no role for the orientation of the magnetization axis

The MCA results obtained using the LSDA and GGA are in most cases different, which led us to the conclusion that there is no general rule favoring either LSDA or GGA for a better description of the MAE of magnetic alloys. The calculated orbital moment anisotropy is similar for both LSDA and GGA and cannot explain the differences in the calculation of the MCA. Nevertheless, from this paper it seems that the LSDA results are slightly in better agreement with the available experimental results. To confirm this claim further experimental data are needed.

## ACKNOWLEDGMENTS

We thank J. M. Wills for providing us with his FPLMTO code. I.G. was supported by an European Union Grant No. ERBFMXCT96-0089. Calculations were performed using both the SGI Origin-2000 supercomputer of the Université Louis Pasteur de Strasbourg and that of CINES under Grant No. gem1917.

<sup>1</sup>B.M. Lairson and B.M. Clemens, Appl. Phys. Lett. **63**, 1438 (1993).

<sup>2</sup>G.H.O. Daalderop, P.J. Kelly, and M.F.H. Schuurmans, Phys. Rev. Lett. **71**, 2165 (1993).

<sup>3</sup>H.J.G. Draaisma and W.J.M. de Longe, J. Appl. Phys. **64**, 3610 (1988).

<sup>4</sup>L. Néel, J. Phys. Radium **15**, 225 (1954).

<sup>5</sup>P. Bruno, *Physical Origins and Theoretical Models of Magnetic Anisotropy* (Ferienkurse des Forschungszentrum Jülich, Jülich, 1993).

<sup>6</sup>S.S.A. Razee, J.B. Staunton, and F.J. Pinski, Phys. Rev. B **56**, 8082 (1996).

<sup>7</sup>S.S.A. Razee, J.B. Staunton, F.J. Pinski, B. Ginatempo, and E. Bruno, J. Appl. Phys. **83**, 7097 (1998).

<sup>8</sup>S.S.A. Razee, J.B. Staunton, B. Ginatempo, F.J. Pinski, and E. Bruno, Phys. Rev. Lett. **82**, 5369 (1999).

<sup>9</sup>W. Grange, thesis, Université Louis Pasteur, Strasbourg, 1998; W. Grange, I. Galanakis, M. Alouani, M. Maret, J.-P. Kappler, and A. Rogalev, Phys. Rev. B **62**, 1157 (2000).

<sup>10</sup>P. Bruno, Phys. Rev. B **39**, 865 (1989).

<sup>11</sup>G. van der Laan, J. Phys.: Condens. Matter **10**, 3239 (1998).

<sup>12</sup>J.M. Wills and B.R. Cooper, Phys. Rev. B **36**, 3809 (1987); M. Alouani and J.M. Wills, *ibid.* **54**, 2480 (1996); J. Wills, O. Eriksson, M. Alouani, and D.L. Price, *Electronic Structure and*

*Physical Properties of Solids: The Uses of the LMTO Method*, edited by Hugues Dreyssé, Lecture Notes on Physics, Vol. 535 (Springer-Verlag, New York, 2000).

<sup>13</sup>H.J.F. Jansen, Phys. Rev. B **38**, 8022 (1988).

<sup>14</sup>P. Hohenberg and W. Kohn, Phys. Rev. **136**, B864 (1964); W. Kohn and L.J. Sham, *ibid.* **140**, A1133 (1965).

<sup>15</sup>U. von Barth and L. Hedin, J. Phys. C **5**, 1629 (1972).

<sup>16</sup>J.P. Perdew and Y. Wang, Phys. Rev. B **33**, 8800 (1986); **45**, 13 244 (1992).

<sup>17</sup>P. Villars and L.D. Calvet, *Pearson's Handbook of Crystallographic Data for Intermetallic Phases* (American Society for Metals, Metals Park, OH, 1985).

<sup>18</sup>K. Takahashi, S. Mitani, M. Sano, H. Fujimori, H. Nakajima, and A. Osawa, Appl. Phys. Lett. **67**, 1016 (1995).

<sup>19</sup>P. Kamp, A. Marty, B. Gilles, R. Hoffmann, S. Marchesini, M. Belakhovsky, C. Boeglin, H.A. Dürr, S.S. Dhesi, G. van der Laan, and A. Rogalev, Phys. Rev. B **59**, 1105 (1999).

<sup>20</sup>E.T. Kulatov, Yu.A. Uspenskii, and S.V. Halilov, J. Magn. Magn. Mater. **163**, 331 (1996).

<sup>21</sup>T. Tohyama, Y. Ohta, and M. Shimizu, J. Phys.: Condens. Matter **1**, 1789 (1989).

<sup>22</sup>R.J. Lange, S.J. Lee, D.W. Lynch, P.C. Canfield, D.N. Harmon, and S. Zollner, Phys. Rev. B **58**, 351 (1998).

<sup>23</sup>J. Kübler, J. Magn. Magn. Mater. **45**, 415 (1984).

<sup>24</sup>I.V. Solovyev, P.H. Dederichs, and I. Mertig, Phys. Rev. B **52**, 13 419 (1995).

- <sup>25</sup> A. Sakuma, *J. Phys. Soc. Jpn.* **63**, 3053 (1994).
- <sup>26</sup> O.K. Andersen, *Phys. Rev. B* **12**, 3060 (1975).
- <sup>27</sup> A.R. Macintosh and O.K. Andersen, in *Electrons at the Fermi Surface*, edited by M. Springfold (Cambridge University Press, Cambridge, 1980)
- <sup>28</sup> P. Oppeneer, *J. Magn. Magn. Mater.* **188**, 275 (1998).
- <sup>29</sup> P. Ravindran, A. Kjekshus, H. Fjellvag, P. James, L. Nordström, B. Johansson, and O. Eriksson (unpublished); P. James, thesis, Uppsala University, Uppsala, 1999.
- <sup>30</sup> P. Eurin and J. Pauleve, *IEEE Trans. Magn.* **5**, 216 (1969).
- <sup>31</sup> J.-U. Thiele, L. Folks, M.F. Toney, and D.K. Weller, *J. Appl. Phys.* **84**, 5686 (1998).
- <sup>32</sup> O.A. Ivanov, L.V. Solina, V.A. Demshina, and L.M. Magat, *Fiz. Met. Metalloved.* **35**, 92 (1973).
- <sup>33</sup> G.H.O. Daalderop, P.J. Kelly, and M.F.H. Schuurmans, *Phys. Rev. B* **44**, 12 054 (1991).
- <sup>34</sup> W. Grange, M. Maret, J.-P. Kappler, J. Vogel, A. Fontaine, F. Petroff, G. Krill, A. Rogalev, J. Goulon, M. Finazzi, and N.B. Brookes, *Phys. Rev. B* **58**, 6298 (1998).
- <sup>35</sup> G. Armelles, D. Weller, B. Rellinghaus, P. Caro, A. Cebollada, and F. Briones, *J. Appl. Phys.* **82**, 4449 (1997); L. Creveling, H.L. Luo, and G.S. Knapp, *Phys. Rev. Lett.* **18**, 851 (1967); R.S. Toth, A. Arrit, S.S. Shimozaki, S.A. Werner, and H. Sato, *J. Appl. Phys.* **40**, 1373 (1969).
- <sup>36</sup> I. Osterloh, P.M. Oppeneer, J. Sticht, and J. Kübler, *J. Phys.: Condens. Matter* **6**, 285 (1994).
- <sup>37</sup> A. Kootte, C. Haas, and R.A. de Groot, *J. Phys.: Condens. Matter* **3**, 1133 (1991).
- <sup>38</sup> B. van Laar, *J. Phys. (France)* **25**, 600 (1964).
- <sup>39</sup> V. Cros, F. Petroff, J. Vogel, A. Fontaine, J.-P. Kappler, G. Krill, A. Rogalev, and J. Goulon, *J. Appl. Phys.* **81**, 3774 (1997).
- <sup>40</sup> R. Wu, D. Wang, and A.J. Freeman, *Phys. Rev. Lett.* **71**, 3581 (1993); R. Wu and A.J. Freeman, *ibid.* **73**, 1994 (1994).
- <sup>41</sup> V.L. Moruzzi and P.M. Marcus, *Phys. Rev. B* **48**, 16 106 (1993).
- <sup>42</sup> Y. Nakata, M. Yoshikawa, and Y. Hirotsu, *J. Magn. Magn. Mater.* **177-181**, 1175 (1998).
- <sup>43</sup> P.M. Oppeneer, I. Galanakis, P. James, O. Eriksson, and P. Ravindran, *J. Magn. Soc. Jpn.* **23**, 21 (1999).
- <sup>44</sup> P.M. Oppeneer, V.N. Antonov, T. Kraft, H. Eschrig, A.N. Yaresko, and A.Ya. Perlov, *J. Phys.: Condens. Matter* **8**, 5769 (1996).
- <sup>45</sup> K. Iwashita, T. Oguchi, and T. Jo, *Phys. Rev. B* **54**, 1159 (1996).
- <sup>46</sup> F. Menzinger and A. Paoletti, *Phys. Rev.* **143**, 365 (1966).
- <sup>47</sup> S.J. Pickart and R. Nathans, *J. Appl. Phys.* **33**, S1336 (1962).
- <sup>48</sup> M. Auwärter and A. Kussmann, *Ann. Phys. (N.Y.)* **7**, 169 (1950).
- <sup>49</sup> B. Antonini, F. Lucari, F. Menzinger, and A. Paoletti, *Phys. Rev.* **187**, 611 (1969).
- <sup>50</sup> K. Adachi, M. Matsui, and Y. Fukuda, *J. Phys. Soc. Jpn.* **48**, 62 (1980).
- <sup>51</sup> M. Yessik, J. Noakes, and H. Sato, *J. Appl. Phys.* **42**, 1349 (1971).
- <sup>52</sup> I. Galanakis, P.M. Oppeneer, P. Ravindran, L. Nordström, P. James, M. Alouani, H. Dreyssé, and O. Eriksson (unpublished).